Electron capture β decay of ^{7}Be encapsulated in C_{60}: Origin of increased electron density at the ^{7}Be nucleus

E. V. Tkalya,[1,2,*] A. V. Bibikov,[1] and I. V. Bodrenko[1]

[1]*Skobeltsyn Institute of Nuclear Physics, Lomonosov Moscow State University, Leninskie gory, Moscow, 119991, Russia*

[2]*National Institute for Theoretical Physics, Stellenbosch Institute of Advanced Study, Private Bag X1, Matieland 7602, South Africa*

(Received 4 September 2009; revised manuscript received 12 January 2010; published 24 February 2010)

We offer a new theoretical interpretation for the effect of enhanced electron density at the ^{7}Be nucleus encapsulated in fullerene C_{60}. Our *ab initio* Hartree-Fock calculations show that the electron density at the ^{7}Be nucleus in ^{7}Be@C_{60} increases due to the attractive effective potential well generated by the fullerene. The $2s$ state in the isolated Be atom turns into a $3s$ state in the joint potential. This new state has higher energy and slightly larger amplitude at the Be nucleus than the previous $2s$ state. Moreover the $3s$ wave function has an additional node that appeared at a distance $r \simeq 5a_B$ from the center. The node imitates repulsion between the Be electron and the fullerene wall because the electron has zero probability to occupy this region. Such an imitation of the repulsion by means of the node in an attractive potential has a direct physical analogy in the theory of α-α and N-N nuclear interactions.

DOI: 10.1103/PhysRevC.81.024610 PACS number(s): 21.10.Tg, 23.40.Hc, 27.20.+n, 36.40.Cg

I. INTRODUCTION

In the ^{7}Be β decay via the electron capture (EC) process, the nucleus absorbs an electron from the atomic or molecular shell and is transformed to ^{7}Li in the reaction $p + e^- \rightarrow n + \nu_e$. The decay rate is proportional to the electron density at the nucleus and therefore depends on the chemical environment of the radioactive isotope. ^{7}Be was used in investigations of the EC decay rate in various chemical states since the first studies by Segre [1] and Daudel [2]. By now, experimentalists have published the results of more than 60 measurements relating to K and L-shell EC by ^{7}Be in different chemical forms and media.

From 2005 to 2007, two teams studied the EC decay of ^{7}Be inside the fullerene C_{60} [3–5]. It was found that the half-life of ^{7}Be in metallic Be measured at room temperature exceeds the one in ^{7}Be@C_{60} at room temperature by 0.83% [3] and by 1.5% [5] if the latter is measured at 5°K. This difference between the ^{7}Be EC β-decay constants is the largest among available experiments. A density functional theory (DFT) basing numerical calculations of the electron density at the Be nucleus was presented in Refs. [5,6] along with the experimental data. It was found that, in accordance with the experiment, the electron density at Be encapsulated in the center of C_{60} is larger than the one at the nuclei in metallic Be. Qualitatively, in the metal the electrons are shared, decreasing their local density at the nuclei, while the Be atom in C_{60} remains intact. A more careful analysis, however, showed that the electron density at ^{7}Be@C_{60} is larger by 0.17% even in comparison with that in an isolated Be atom. The authors explain this result as a "compression" of the Be's $2s$ orbital inside C_{60}. The reason for the compression may be the "repulsive interaction" between Be and the C_{60} cage according to Ref. [7].

*tkalya@srd.sinp.msu.ru

II. EXAMINATION WITHIN THE FRAMEWORK OF HARTREE-FOCK BASED METHODS

A detailed understanding of the structure of atoms encapsulated in fullerenes is important, in particular, for developing the concept of the fullerene as an isolating cage, which "does not affect" the trapped single atom and "protects" it from the outer environment. In the present work, we study the Be-C_{60} interaction and its effect on the electron density at the Be nucleus within the framework of Hartree-Fock (HF)-based methods. Although our value of the relative decay-rate difference between metallic Be and Be@C_{60} is in qualitative agreement with the experimental one as well as with the results of the previous theoretical studies, we suggest a new theoretical interpretation of the physical nature of the enhanced electron density at Be in C_{60}.

We started with the structural optimization of the Be position inside C_{60}. The fullerene's geometry was taken from the experiment in Ref. [8] (the length of the long and the short bonds are 1.448 and 1.404 Å, respectively) and fixed during the optimization, as the endohedral doping has, as expected, a small effect [7]. The total energy of the Be@C_{60} complex at every trial configuration was calculated by the restricted (singlet spin state) HF method, with the 6-31G** molecular basis set [9,10] in a Cartesian form. In addition, the electronic correlations were taken into account within the second-order perturbation method (MP2). For the calculations we used our original program, which employs the resolution of the identity (RI) method for the electron-electron interaction integrals and allows us to perform the HF-based calculations for large systems with moderate computational resources (see Refs. [11,12] for details). For both the HF and the MP2 variants, the optimization results in the position of the Be atom at the center of the fullerene are in full agreement with the previous DFT-based studies [5,7]. To evaluate the interaction energy defined as $\Delta E = E_{\mathrm{Be@C_{60}}} - (E_{\mathrm{Be}} + E_{\mathrm{C_{60}}})$, we performed additional calculations of the total energies of the Be atom E_{Be} and the fullerene $E_{\mathrm{C_{60}}}$. In addition, in a

TABLE I. The Be-C_{60} interaction energy in eV (Be is at the center of the fullerene).

	HF	HF + MP2
CP corrected	0.91	−0.41
Uncorrected	1.00	−0.63

separate calculation, the basis set superposition error was taken into account by the counterpoise (CP) method [13]. The results are summarized in Table I.

We therefore conclude that the Be atom's equilibrium position at the center of the fullerene belongs to the attractive region of the van der Waals interaction (i.e., the Be-C_{60} interaction is attractive and the Be@C_{60} complex is stable in the ground state with respect to the decay to Be and C_{60}). This result is in contrast with the one of Lu *et al.* [7] who concluded a "slightly repulsive" Be-C_{60} interaction from a DFT calculation and obtained the value of +1.05 eV for the interaction energy. We apply their speculations to our HF results, which also give the repulsive interaction as the pure HF method may not account for the dispersion energy.

The consideration of Lu *et al.* is based on the modifications in the energy levels of the highest occupied/lowest unoccupied molecular orbitals (HOMO/LUMO) of the Be atom and C_{60} upon the formation of the Be@C_{60} complex. Our results, presented in Fig. 1, differ qualitatively from those of Ref. [7], calculated with the B3LYP density functional with the 6-31G** molecular basis set. In Ref. [7], Be's atomic 2*s* level lies in the middle of C_{60}'s HOMO/LUMO gap. Moreover, C_{60}'s HOMO/LUMO gap increases in Ref. [7] upon endohedral doping with Be because the HOMO is slightly lowered by 0.03 eV while the LUMO is elevated by 0.04 eV. These results were interpreted by Lu *et al.* as the evidence of a slight repulsion between the Be atom and the fullerene cage in the Be@C_{60} complex. Our calculations show that the Be's 2*s* orbital in the Be@C_{60} complex lies 0.14 eV lower than the C_{60}'s HOMO (see Fig. 1). (The Be's 2*s* orbital in isolated Be atom lies 0.69 eV lower than the C_{60}'s HOMO.) Furthermore, C_{60}'s HOMO/LUMO gap does not change upon the endohedral doping and both orbitals are just slightly lowered by 0.01 eV. Thus, there is little evidence of the "repulsive interaction," according to the definition of Lu *et al.* between Be and C_{60} within the HF calculations, even if the calculated interaction energy is positive.

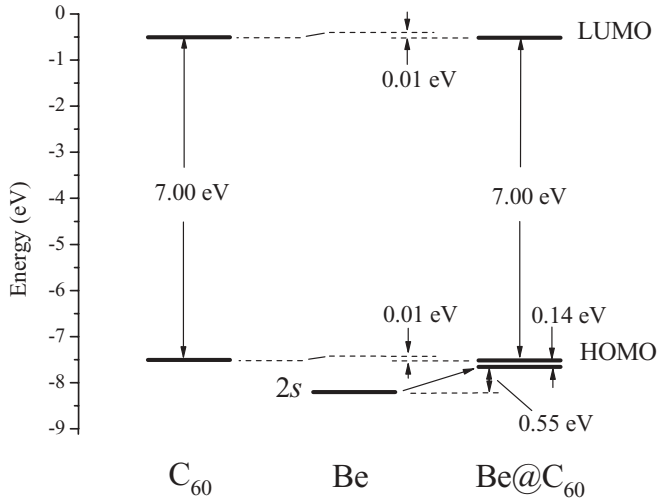

FIG. 1. Energy levels of molecular orbitals in C_{60}, Be atom, and Be@C_{60}.

The Mulliken population analysis of our HF calculations with the 6-31G** molecular basis set gives the charge of +0.03 at Be compared with −0.14 in the DFT calculation of Lu *et al.* with the same basis set. This makes the concept of a slight hybridization between Be and the fullerene orbitals unacceptable within the HF method. However, strictly speaking, the Mulliken charges are not suitable basis set independent parameters for analyzing the nonchemical interactions.

Then, we consider the local electron density at the Be nucleus. The electron density for a polyatomic system is given by the standard relation $\rho(\mathbf{r}) = \Sigma_n \kappa_n |\varphi_n(\mathbf{r})|^2$, where $\varphi_n(\mathbf{r})$ are normalized molecular orbitals κ_n—corresponding occupation numbers. In our case, the orbitals are the HF orbitals calculated with Danning's correlation-consistent polarized valence-only double-zeta (cc-pVTZ) molecular basis set [14] used in a Cartesian form. We employed two methods for the evaluation of the electron density at the nucleus that is formally located at the coordinate origin $r = 0$. At first we added narrow Gaussian *s* functions (with exponents α between 10^3 and 10^8 in the inverse-squared Bohr radius a_B^{-2}) to the standard basis set. Then we extrapolated the local electron density near the nucleus to the $r = 0$ point by using the known (the consequence of the Kato theorem [15]) nonrelativistic asymptotic of the electron density for a many-electron system at the Coulomb center with charge Z, $[d\rho(r)/dr]_{r=0} = -2Z\rho(0)$. The coincidence of both values of the electron density at the Be nucleus with up to 0.02 a.u. (the atomic unit of density is equal to one electron in the cubic Bohr radius a_B^{-3}), about 0.05%, reflects the level of numerical error for our method. The calculated electron densities at a single Be atom, metallic Be, and Be@C_{60} are summarized in Table II. (Details of the procedures for calculations of electron density at metallic Be will be presented elsewhere.)

Our results show that

$$\frac{\rho(0)_{\mathrm{Be@C_{60}}} - \rho(0)_{\mathrm{Be\ metal}}}{\rho(0)_{\mathrm{Be\ metal}}} 100\% \simeq 2.0\%,$$

that is, a 2% decrease of the electron density at the nucleus from Be@C_{60} to metallic Be that is in qualitative agreement with the experimentally determined change of the decay rate at 5°K. Though the absolute value is somewhat larger then the measured 1.5% as well as the value of 1.7% obtained by

TABLE II. Calculated electron density (in a.u.) at the Be nucleus.

	Orbitals			
	1st	2nd	Others	Total
Be@C_{60}	34.22	1.24	0.02	35.48
Be atom	34.25	1.13	–	35.38
Be metal	34.11	0.32	0.33	34.78

the DFT calculations [5,6]. However, our value is in excellent agreement with the experimental data of Kraushaar *et al.* [16] of the direct measurement of the ^{7}Be half-life in the metal source $T_{1/2}^{^7\text{Be metal}} = 53.61 \pm 0.17$ days and the half-life of ^{7}Be in ^{7}Be@C_{60} $T_{1/2}^{^7\text{Be@C}_{60}} = 52.47 \pm 0.04$ days from the work of Ref. [5]

$$\frac{T_{1/2}^{^7\text{Be metal}} - T_{1/2}^{^7\text{Be@C}_{60}}}{T_{1/2}^{^7\text{Be metal}}} 100\% \simeq 2.1\%.$$

In the present article we do not discuss these minor quantitative discrepancies neither between available experimental data nor between various theoretical results. The experimental data require further specification. As to numerical results, it is necessary to take into account that both methods of calculation contain approximations. The HF method correctly takes account of the exchange, but lacks for the electronic correlations. The model density functionals, however, make approximations for both the exchange and the correlations. To make a reasoning about the accuracy of the methods, especially in the case of the nonchemically, weakly bounded molecules, one will refer to more robust theories such as the coupled clusters or the configuration interaction methods. Instead, we are focusing on a qualitative phenomenon—the electron density difference between Be@C_{60} and an isolated Be atom. The corresponding relative decrease of the electron density in our calculations is 0.28%, in qualitative accord with the value of 0.17% in Refs. [5,6]. The reason for the enhanced electron density in Be@C_{60} might be a slight hybridization of Be's and C_{60}'s orbitals, as suggested in Ref. [7], so that the Be grabs the electron density from the fullerene. In that case, some of the fullerene's orbitals will contribute to the electron density at Be. However, only two orbitals (those originated from atomic 1s and 2s) make an apparent contribution to the electron density at the Be nucleus. Thus, the hybridization concept has no support from the HF results.

The structure of the Be is therefore changed due to the potential effect of the fullerene. In particular, the fullerene's electrostatic field might prevent the Be's electrons from spreading out the cage acting as a strong repulsive potential wall. In that case, a more compact 1s orbital will not be affected. However, the 2s one will rapidly vanish after a certain distance from the center and will be compressed (due to the normalization) in the internal region resulting in the enhanced density at the nucleus. This concept, which also was expressed in Ref. [5], is in full accord with the data from Table II as well as with the increased energy of the 2s orbital of Be in C_{60}. Nevertheless, a more detailed analysis of the spherically averaged electron density curves for the 1s and 2s orbitals of atomic Be and Be in C_{60} presented on Fig. 2 rules out the concept of a *repulsive* potential wall. Indeed, Be's 2s orbital inside the fullerene tends to zero at $r \simeq 5a_B$, then rapidly increases and becomes even larger than the one of an isolated Be atom. In the following we suggest a different solution to this intriguing issue.

The electron density of the 2s orbital vanishes at $r \simeq 5a_B$ since the corresponding wave function crosses zero and changes its sign. Zero probability for the electrons to occupy the vicinity of $r \simeq 5a_B$ imitates the repulsive core for the 2s

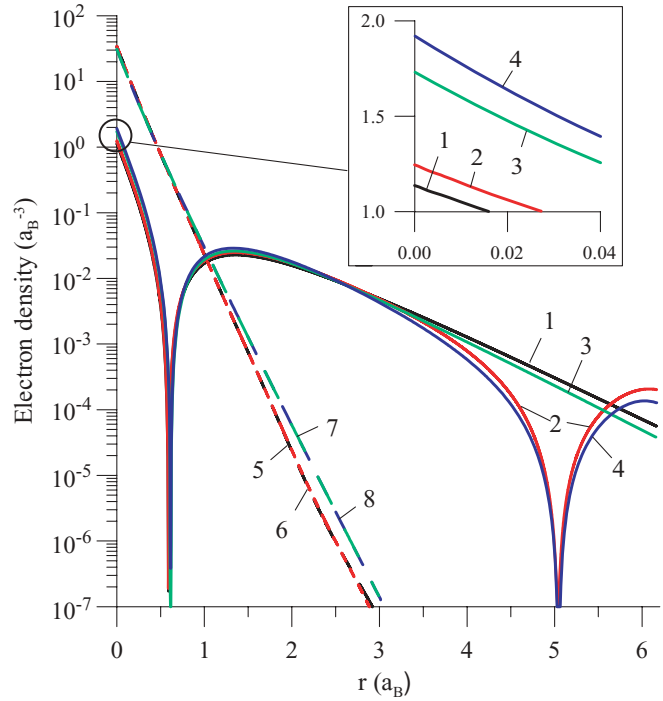

FIG. 2. (Color online) Electron densities of 1s and 2s states for an isolated Be atom and the first and second orbitals of the Be atom in the Be@C_{60} complex: 1 (5): 2s (1s) Be, Hartree-Fock; 2 (6): 2s (1s) Be@C_{60}, Hartree-Fock; 3 (7): 2s (1s) Be@C_{60}, model potential in Figure 3; 4 (8): 2s (1s) Be@C_{60}, model potential with model potential well in Figure 3.

electrons of Be in C_{60}. However, the origin of the additional node in the wave function is the *attractive* potential well at $5a_B \lesssim r \lesssim 8a_B$. A spherically averaged electrostatic potential extracted from the HF electron density of C_{60} (dashed-line curve in Fig. 3) is attractive. To illustrate the phenomenon, we designed a model spherical potential for the 2s orbital of Be (see Fig. 3). It consists of the screened Coulomb potential as well as the spherical attractive potential well centered at $r \simeq 6.7a_B$. The screening constant was chosen to reproduce qualitatively the 2s orbital for the isolated atom. It turns out that the addition of the attractive potential into the model potential results in the appearance of the second node for the 2s orbital, in the increase of its energy (in full agreement with the result of HF calculation, see Fig. 1), and also in the increase of the electron density at $r = 0$.

III. ANALYTICALLY SOLVABLE MODEL

The reason for this phenomenon becomes clear from the following analytically solvable model. Let us compare the 2s and 3s electron wave functions and the energy levels in the Coulomb potential [Fig. 4(a)] and in the new potential shown in Fig. 4(b). (This is the same Coulomb potential combined with the spherical potential layer.)

We consider here only s wave functions $\varphi_{ns}(r)$ because $\varphi_{np}(0) = 0$ for all p states in the nonrelativistic limit and these p states do not give a contribution to the decay of ^{7}Be. The

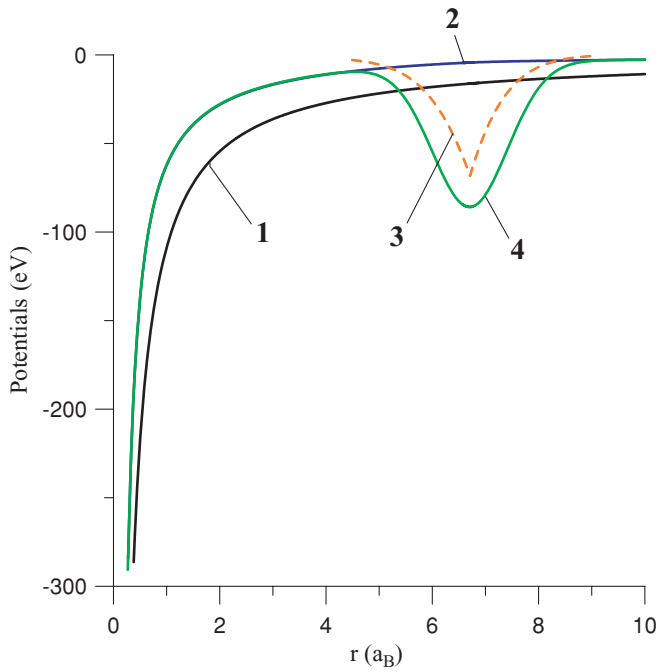

FIG. 3. (Color online) Potentials for the Be $2s$ orbital in the Be@C_{60} complex: 1: Coulomb potential; 2: model potential (screened Coulomb potential); 3: potential well extracted from Hartree-Fock electron density; 4: model potential "2" with model potential well.

electron radial wave functions for the combined potential in Fig. 4(b) are

$$\varphi_s(r) = \begin{cases} a_1 \exp(-\kappa r)\,{}_1F_1(1 - Z/\kappa; 2; 2\kappa r), & 0 \leqslant r < R_1, \\ a_2(\sin(kr) + b_2 \cos(kr))/r, & R_1 \leqslant r < R_2, \\ a_3 \exp(-\kappa r)/r, & R_2 \leqslant r. \end{cases}$$

Here, ${}_1F_1$ is the confluent hypergeometric function, the wave numbers are $\kappa = \sqrt{2m|E|}$ and $k = \sqrt{2m(E - V)}$, where E is the energy of the state ($E, V < 0$). The coefficients a_{1-3}, b_2, and the energy E are determined from the conditions of continuity and differentiability of the wave function at the boundaries $r = R_1$ and $r = R_2$, where $R_{1,2}$ are the internal and external radii of the potential layer, respectively.

For definiteness, we take charge $Z = 2$ for the Coulomb potential and depth $V = -50$ eV for the spherical layer located between $R_1 = 5.5$ a_B and $R_2 = 7.5$ a_B. The energy and the electron density at the nucleus of the $2s$ state in this potential are $E_{2s} = -13.61$ eV and $\rho_{2s}(0) = 4$ a_B^{-3}, respectively. If we add the spherical potential layer to the Coulomb potential, as is shown in Fig. 4(b) and gradually increase its depth up to the value of 50 eV, we will see the following. The energy of the $2s$ state decreases; its wave function gradually moves from the region of the Coulomb potential to the region of the spherical layer and becomes similar to the wave function of the $1s$ state in the isolated potential layer shown in Fig. 4(c). The electron density of the $2s$ state at the nucleus decreases according to Fig. 5. At the same time the $3s$ state gradually takes up the space region occupied previously by the $2s$ state. Depending on the width of the spherical potential layer and on its depth V, the energy of the $3s$ state in the new combined potential may lie both above and below the $2s$ energy level in the Coulomb potential and may have either a higher or a smaller electron density at the nucleus (see Fig. 5).

Qualitatively, the mechanism of the variation of the electron density of the $3s$ state at the nucleus, shown in Fig. 5, follows. The electron density in the origin $\rho_{ns}(0)$ depends on the energy of the state E_{ns}. For example, $\rho_{ns}(0) \propto |E_{ns}|^{3/2}$ in the Coulomb potential, $\rho_{ns}(0) \propto |E_{ns}|$ in the infinite potential well, and so on. The absolute value of the energy $|E_{3s}|$ of the $3s$ state increases when the depth $|V|$ of the spherical potential layer grows. At the same time, a gradual redistribution of the $3s$ electronic density between the area of the Coulomb potential and the spherical potential layer starts. For a relatively small $|V|$, the space occupied by the $3s$ wave function in the area of the potential spherical layer increases comparatively slowly because the area of localization of the wave function practically does not vary and the spherical potential layer does not have its own binding state. If the layer has a large depth the situation changes. There is a binding state in the deep isolated spherical potential layer now. The energy of the $3s$ state in the joint potential verges toward the energy of such a binding state, moving simultaneously from the position of the binding state in the pure Coulomb field. A part of the wave function occupies the forbidden-for-classical-movement area (between the Coulomb potential and the spherical potential layer) and the considerable enhancement of the $3s$ electron density occurs in the area of the spherical potential layer. The reduction of the wave function in the area of the Coulomb potential is no longer compensated by the growth of the $|E_{3s}|$ energy and the electronic density at the nucleus decreases rapidly, returning at first to the initial value (see Fig. 5), and tends to zero at the further increase of the spherical potential layer depth.

By applying the previous considerations to the Be@C_{60} system one concludes the following. The C_{60} fullerene modifies the Coulomb potential of the Be atom in such a way that the $3s$ state in the joint potential occupies approximately the same position as the $2s$ state in the isolated Be atom. That is, the $3s$ state has approximately the same energy and practically the same electron density inside the Be atom as the $2s$ state in the Coulomb potential. Moreover, the corresponding wave function $\varphi_{3s}(r)$ has the second node, which imitates the repulsion of the electrons of the Be atom from the C_{60} cage at $r \simeq 5a_B$. As regarding the Be $2s$ state, the energy of this state becomes considerably smaller in the new potential. Furthermore, its wave function moves to the potential well formed by the fullerene.

In that way, the small increase of the electron density at the Be nucleus has a casual character. One can obtain another result with different parameters of the "fullerene potential well" (for example, by doping of C_{60} with certain atoms). Thus, we obtain an infrequent possibility to control the ^{7}Be decay by means of a nonchemical interaction. In the considered particular case, this is the electrostatic interaction between the Be atom and the fullerene.

To confirm that the proposed mechanism does not depend on the model, we also considered two different analytically solvable models—a particle inside two "independent" and two connected spherical potential wells. The results obtained are in good qualitative agreement with those described previously.

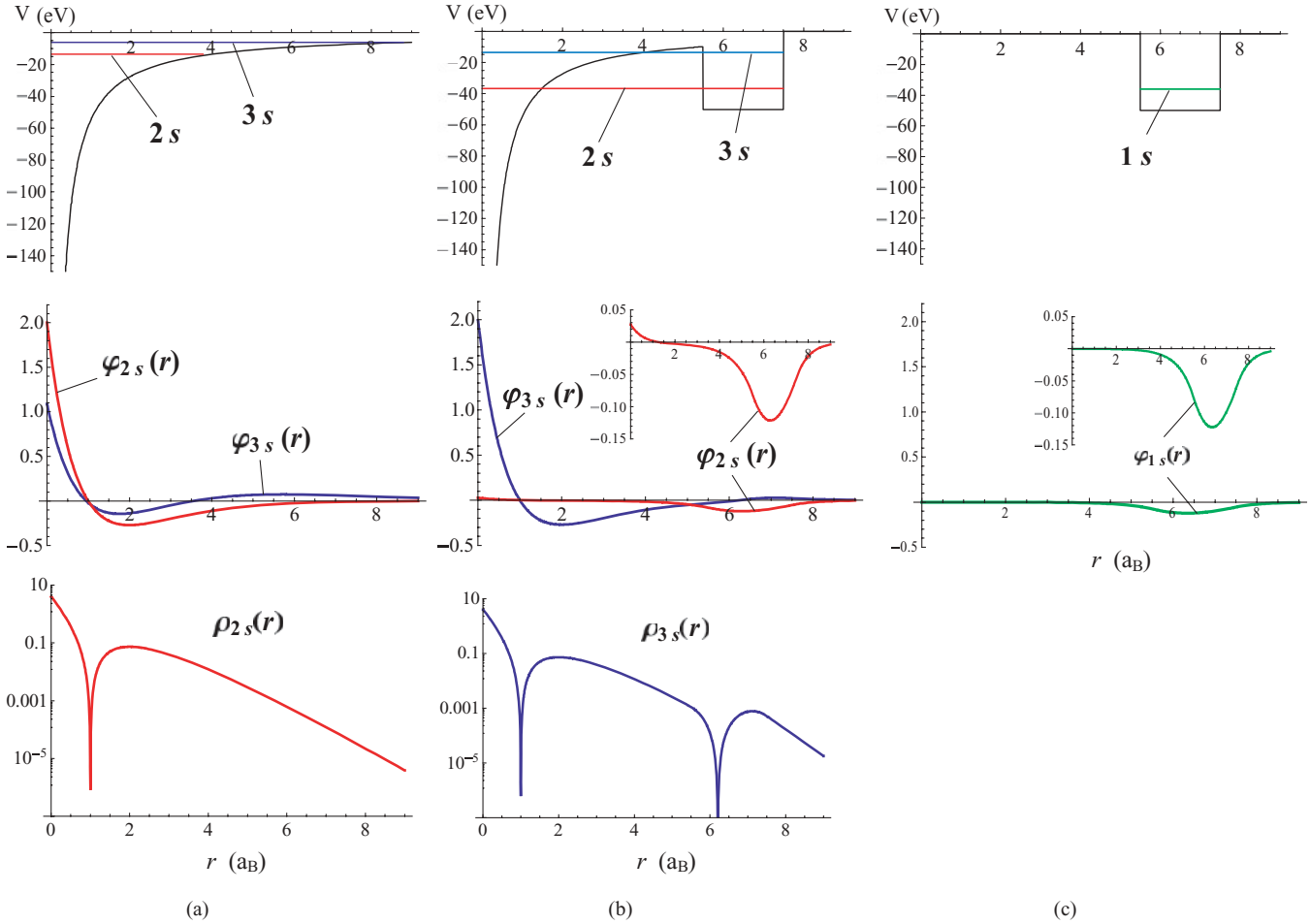

FIG. 4. (Color online) Energy levels, electron wave functions, and electron densities of 2s and 3s states in: (a) Coulomb potential and (b) Coulomb potential combined with a spherical potential layer. (c) Energy level and electron wave function of 1s state in a single spherical potential layer.

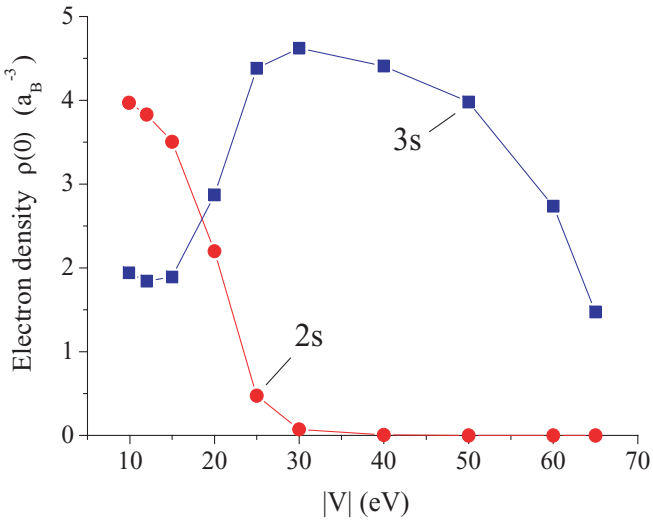

FIG. 5. (Color online) Electron densities of 2s and 3s states at the point $r = 0$ as a function of spherical potential layer depth V.

IV. COMPARISON WITH REPULSIVE CORE IN α-α AND N-N INTERACTIONS

It is interesting to note in the end that the problem considered here is not physically new and has a vague similarity with the well-known problem of the repulsive core in nuclear physics. The concept of a repulsive core in α-α and N-N interactions was accepted as correct right until the 1970's. This repulsive core arose at small distances as the consequence of the Pauli exclusion principle. It was established later that this concept was simplified. In some cases, the repulsive core must be understood in terms of the nodal wave function for relative motion in an attractive potential (see Refs. [17,18] and references therein).

In other words, the zero probability for a particle to occupy a certain region can be achieved both by the infinite potential wall (repulsive core) and by the node of the wave function in an attractive potential. In this sense the phenomenon considered in the present article resembles the previously mentioned effects in the α-α and the N-N interactions.

V. CONCLUSION

In summary, according to our HF calculations with the electronic correlations accounted at the MP2 level, the lowest

energy singlet configuration of the Be atom encapsulated in C_{60} is the one at the center of the fullerene—in accordance with the previous DFT studied. The Be atom resides in the attractive region of the van der Waals interaction with the interaction energy of about -0.6 eV—in contrast with $+1.05$ eV from the DFT. Thus, the ^{7}Be@C_{60} complex is stable with respect to the decay to ^{7}Be and C_{60}. The HF electron density at the Be nucleus in Be@C_{60} exceeds the one in metallic Be by 2%, in qualitative agreement with the relative difference of the corresponding ^{7}Be EC decay rates measured by Ohtsuki *et al.* [5] as well as with the DFT calculations. The electron density at the Be nucleus in ^{7}Be@C_{60} also exceeds the one in an isolated Be atom. The origin of this increase is neither the modification of the Be's $2s$ orbital in C_{60} because of the hybridization with the fullerene orbitals nor the repulsive potential wall at the region of the fullerene's atoms. Rather the replacement of the Be $2s$ state by the $3s$ orbital in the new potential, which is the joint Coulomb potential of the Be atom and the attractive effective potential well generated by the fullerene. The $3s$ state has an additional node at a distance $r \simeq 5a_B$ from the center. This node imitates the repulsion between electrons of the Be atom and the C_{60} cage, which has a direct physical analogy in the theory of α-α and N-N nuclear interactions.

ACKNOWLEDGMENTS

E. Tkalya thanks Prof. Frederik Scholtz and Dr. Alexander Avdeenkov for the hospitality and for the given opportunity to do a part of this work at the National Institute for Theoretical Physics, South Africa.

[1] E. Segre, Phys. Rev. **71**, 274 (1947).
[2] R. Daudel, La Revue Scientifique, Paris **85**, 162 (1947).
[3] T. Ohtsuki, H. Yuki, M. Muto, J. Kasagi, and K. Ohno, Phys. Rev. Lett. **93**, 112501 (2004).
[4] A. Ray *et al.*, Phys. Rev. C **73**, 034323 (2006).
[5] T. Ohtsuki, K. Ohno, T. Morisato, K. Ohno, T. Morisato, T. Mitsugashira, K. Hirose, H. Yuki, and J. Kasagi, Phys. Rev. Lett. **98**, 252501 (2007).
[6] T. Morisato, K. Ohno, T. Ohtsuki, K. Hirose, M. Sluiter, and Y. Kawazoe, Phys. Rev. B **78**, 125416 (2008).
[7] J. Lu, Y. Zhou, X. Zhang, and X. Zhao, Chem. Phys. Lett. **352**, 8 (2002).
[8] R. D. Johnson, G. Meijer, J. R. Salem, and D. S. Bethune, J. Am. Chem. Soc. **113**, 3619 (1991); W. I. F. David *et al.*, Nature (London) **353**, 147 (1991); A. K. Soper *et al.*, J. Phys.: Condens. Matter **4**, 6087 (1992).
[9] M. M. Francl *et al.*, J. Chem. Phys. **77**, 3654 (1982).
[10] Basis sets were taken from the Extensible Computational Chemistry Environment Basis set Database, Version 02/02/06 (EMSL), http://www.emsl.pnl.gov/forms/basisform.html. Current version of the database is at https://bse.pnl.gov/bse/portal.
[11] A. Artemyev, A. Bibikov, V. Zayets, and I. Bodrenko, J. Chem. Phys. **123**, 024103 (2005).
[12] A. V. Nikolaev, I. V. Bodrenko, and E. V. Tkalya, Phys. Rev. A **77**, 012503 (2008).
[13] S. F. Boys and F. Bernardi, Mol. Phys. **19**, 553 (1970).
[14] T. H. Dunning Jr., J. Chem. Phys. **90**, 1007 (1989).
[15] T. Kato, Commun. Pure Appl. Math. **10**, 151 (1957); E. Steiner, J. Chem. Phys. **39**, 2365 (1963).
[16] J. J. Kraushaar, E. D. Wilson, and K. T. Bainbridge, Phys. Rev. **90**, 610 (1953).
[17] S. Saito, Prog. Theor. Phys. **41**, 705 (1969); V. G. Neudatchin, V. I. Kukulin, V. L. Korotkikh, and V. P. Korennoy, Phys. Lett. **B34**, 581 (1971).
[18] V. G. Neudatchin, I. T. Obukhovsky, Yu. F. Smirnov, and E. V. Tkalya, Z. Phys. A **313**, 357 (1983).